

A Study On Assessment Of Theories For Contact Stress Distribution At Roller- Work Piece Contact In Roller Burnishing

P.Saritha

Abstract— Surface finish is a characteristic of any machined surface. Increasing attention is being paid to the quality of the surface finish obtained in present day products. Residual stresses are developed during the machining processes which are required to be estimated to ensure that there is no distortion induced over a period of time. Also, surface finish has a positive and prolonged effect on the functioning of the machined parts.

Burnishing is a surface modification process, which involves plastic deformation of material at the surface of component due to application a highly polished and hard roller under pressure.

Roller burnishing is used in the present work to get a good surface finish on materials like aluminum and mild steel. This paper discusses the results obtained for contact stresses in a roller burnishing process by using the different theories and numerical methods

Analysis is performed by FEA, ANSYS 13.0. The Results from the analysis are compared with those obtained from different theories and different contact Models of the burnishing process used in the present FEA analysis.

Index Terms—: Roller burnishing, Contact pressure, Finite element method, Hertz theory, single asperity theory, Boresi method.

1. INTRODUCTION

Surface finish is a characteristic of any machined surface. Surface finish is important not only as an appearance but also has a positive and prolonged effect on the functioning of machine parts. In manufacturing engineering it is imperative to attain the desired surface quality in the machine parts in order to ensure their durability. During the operation, the contact stresses on the parts are cyclic in nature and with passage of time lead to sub-surface fatigue cracks.

Burnishing, which is one of the methods to improve surface finish, is also called as chip less finishing process since by applying the forces that exceed the yield strength of the material through hardened roller or ball, the material is cold-worked. This allows the peaks in the surface asperities flow into the valleys. Thus, this process eliminates

grinding and honing while improving the surface finish, surface hardness, wear-resistance, fatigue resistance and corrosion resistance of a part.

Traditionally, Hertz theory has been used to determine the contact stress formed at the interface between two contacting surfaces. Considerable amount of literature exists in the area of burnishing. Earlier researchers who have carried out extensive work in this area include Jawalkar and Walia [1], Eshwar Prasad and Murali Krishna[2] and El-Axir et al [3]. Among others who have worked in this area include Naga malleswara rao et al [4], Lin et al [5], Bouzid et al [6], Nemat et al [7], Safwan et al [8], Hassan, Luo et al [9] and El Tayeb et al [10]. In addition to extensive experimentation, they also tried to establish a theoretical basis for the contact and residual stresses during the burnishing operation. Among the various theories available for determining the residual stresses in the contact zone, the important ones are those proposed by Hertz, Boresi, Single asperity models. In recent times, the finite element method has also been utilized for this purpose [6].

In the present paper, a comparative assessment is made for the residual stresses obtainable by the various above theories. For this purpose, experiments have been carried out in the laboratory on mild steel and Aluminium pieces using roller burnishing operations.

2. DETAILS OF EXPERIMENTATION:

A schematic of the test set-up is given in Fig.1 while the material properties of the work pieces and roller are listed in Table-1. The roller which gets pressed against the work-piece during the operation is mounted in the tool post. In order to measure the load during the operation, the roller is made to transfer the load through to a dial gauge mounted on the tool post.

From a knowledge of the spring constant (obtained through a calibration test) , the load can be obtained as in Table 1.

Load applied on work piece = Total Deflection \times spring constant, where total deflection = Deflection in dial gauge multiplied by the Least count. Least count of the dial gauge used is 0.01mm. Spring constant for spring is 4.3 Kg/mm.

| Material | Length (mm) | Diameter (mm) | Young's modulus (N/mm ²) | Poisson's ratio |
|-------------|-------------|---------------|--------------------------------------|-----------------|
| Mild Steel | 50 | 26 | 2.5×10^5 | 0.27 |
| Aluminum | 50 | 23 | 0.75×10^5 | 0.34 |
| HCHC (Tool) | 10 | 30 | 2.6×10^5 | 0.3 |

Table-1: Material properties of the tool and work piece materials

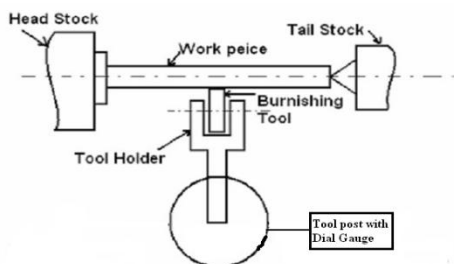


Figure 1: Experimental set-up for burnishing process.

3. THEORIES FOR CONTACT STRESS

2.1 Hertz Theory

Contact stress refers to the localized stresses that develop as two curved surfaces come in contact and deform slightly under the imposed loads and to the stress close to the area of contact between two spheres. Hertz theory gives the contact stress as a function of the normal contact force, the radii of curvature of both bodies and the modulus of elasticity of both bodies. The assumptions made in Hertz contact theory are: a) the strains are small and within the elastic limit, b) each body can be considered an elastic half-space, i.e., the area of contact is much smaller than the characteristic radius of the body, c)

the surfaces are continuous, non-conforming, and d) the surfaces are frictionless.

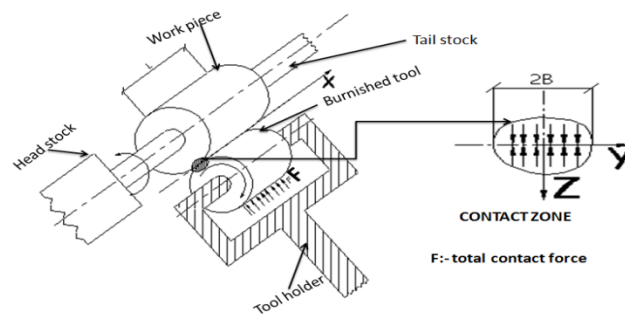


Fig.1. Test set-up used in the experiments

Notations used for the different parameters are:

- D1 = Diameter of Work Piece
- D2 = Diameter of Tool – Roller
- E1 = Young's Modulus of Work Piece
- E2 = Young's Modulus of Roller
- V1 = Poisson's Ratio of Work
- V2 = Poisson's Ratio of Roller
- B = Contact width
- Pmax = Contact pressure

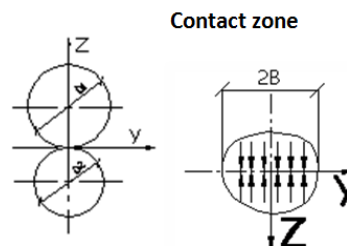


Fig:2 Contact stress between two cylinders

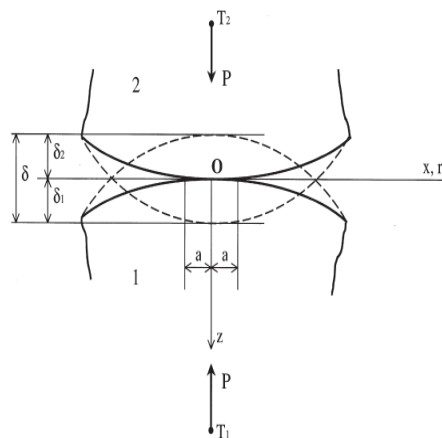


Fig.3:Contact of two nonconforming bodies

$$B = \left\{ \frac{2F [(1-\nu_1^2)/E_1 + (1-\nu_2^2)/E_2]}{\pi L \{(1/D_1) + (1/D_2)\}} \right\}$$

$$P_{max} = \frac{2F}{\pi bL}$$

2.3 Boreasi Method

Boreasi's method [2.3] makes the following assumptions:

- (a) The material of each body is homogenous, isotropic, and elastic in accordance with Hooke's law, but the two bodies are not necessarily made of the same material and b) Shape of surface near point of contact before loading: If the bodies are in the contact at a point, there is a common tangent plane to the surfaces at the point of contact.

In the solution for contact stresses, an expression for the distance between corresponding points on the surfaces near the point of contact is required; corresponding points are points that lie on the surfaces of the bodies and on a line perpendicular to the common tangent plane. Boreasi has presented equations for the stresses at contact zone as follows:

$$B = \sqrt{\frac{2w\Delta}{\pi}}$$

where $W = \frac{\text{force}}{l}$

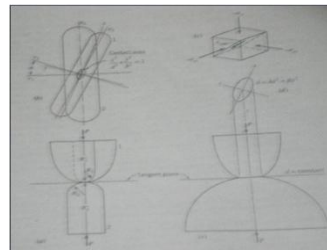
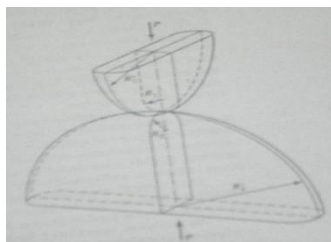


Fig: 4 Analysis of contact stress in Boreasi method [after Boreasi]

Where

$$\Delta = \frac{1}{R_1/2 + R_2/2} \left[\frac{1-\nu_1^2}{E_1} + \frac{1-\nu_2^2}{E_2} \right]$$

ν_1 = Poisson ratio of work piece and R_1 = radius of work piece

ν_2 = Poisson ratio of roller and R_2 = radius of roller

Max. shear stress = $-0.43 \left(\frac{b}{\Delta} \right)$ and Max.

Principal stresses; $k=0$

$$\sigma_{xx} = -b/\Delta; \quad \sigma_{yy} = -2\nu (b/\Delta); \quad \sigma_{zz} = -b/\Delta$$

Shear stress at any point on z-axis is

$$\zeta = \frac{1}{2} (\sigma_{xx} - \sigma_{zz}) \text{ ----- 1}$$

$$\sigma_{xx} = \left[\frac{\left(\sqrt{1 + \left(\frac{z}{b} \right)^2} - \frac{z}{b} \right)^2}{\sqrt{1 + \left(\frac{z}{b} \right)^2}} \right] \frac{b}{\Delta} \quad \& \quad \sigma_{zz}$$

$$= \left[\frac{1}{\sqrt{1 + \left(\frac{z}{b} \right)^2}} \right] \frac{b}{\Delta}$$

$$\sigma_{yy} = -2\nu \left[\sqrt{1 + \left(\frac{z}{b} \right)^2} - \frac{z}{b} \right] \frac{b}{\Delta}$$

We have $\frac{z}{b} = 0.7861$

At this point $\sigma_{xx} = -0.1856 \left(\frac{b}{\Delta} \right)$,

$$\sigma_{yy} = -0.9718 \left(\frac{b}{\Delta} \right), \quad \sigma_{zz} = -0.7861 \left(\frac{b}{\Delta} \right)$$

$$\text{Hence } \zeta_{\max.} = \frac{1}{2} (\sigma_{xx} - \sigma_{zz}) = 0.300 \left(\frac{b}{\Delta} \right)$$

2.2 Single Asperity Model Method

In this method, contact between the two rough solid bodies brought in to contact through the action of applied forces occurs over many small areas, each of which constitutes a single asperity contact. Assumptions in this method are: a) Contact area is elliptical, b) Each body is approximated by an elastic half space loaded over the plane contact area, c) The dimensions of contact area are small compared to the dimensions of each body and to the radius of curvature of the surfaces, d) The strains are sufficiently small for linear elasticity to be valid and e) The contact is frictionless, so that normal pressure is transmit

The point of first contact is taken as the origin of a Cartesian coordinate system with the x - y plane as the common tangent plane and the z -axis directed downwards. Using the notation, normal load P , distant points $T1$ and $T2$ displace distances $d1$ and $d2$ respectively parallel to the z -axis towards O . The quantity $\delta = \delta_1 + \delta_2$ is called the normal approach or the interference.

For the case of solids of revolution, the contact area is circular. The interference, contact radius (a), and maximum contact pressure are given by [2.2]

$$\delta = \left(\frac{9P^2}{16RE^{*2}} \right)^{1/3}, \quad a = \left(\frac{3PR}{4E^*} \right)^{1/3},$$

$$p_0 = \left(\frac{6PE^{*2}}{\pi^3 R^2} \right)^{1/3}, \quad \frac{1}{E^*} \equiv \frac{1-\nu_1^2}{E_1} + \frac{1-\nu_2^2}{E_2}, \quad \frac{1}{R} \equiv \frac{1}{R_1} + \frac{1}{R_2}$$

where p_0 is the maximum contact pressure (which occurs at $r=0$), E^* is the composite Young's modulus, E_1, E_2 and ν_1, ν_2 are the Young's modulus and Poisson's ratios for the lower and upper body respectively, R is the composite radius of curvature and R_1, R_2 are the radii of curvature of the lower and upper bodies respectively. Thus the contact area and the interference each vary as the $2/3$ power of the applied force. The contact pressure distribution is semi-elliptical with radius r and has a maximum value at the origin equal to $3/2$ of the average contact pressure.

Analogous expressions may be written for the contact of two cylindrical bodies whose long axes are parallel to the y -axis. The results for the half-width of the contact strip (a) and the maximum contact pressure are

$$a = \left(\frac{4P'R}{\pi E^*} \right)^{1/2}, \quad p_0 = \left(\frac{P'E^*}{\pi R} \right)^{1/2}$$

where P' is the applied load per unit length of y -direction. The contact pressure distribution is again semi elliptical, this time with a maximum value at the origin equal to $4/\pi$ times the average contact pressure.

2.4. FINITE ELEMENT METHOD:

The numerical determination of stresses in bodies by the finite element method is well known and has been applied to many problems of elasticity, plasticity, creep viscoelasticity and vibrations. While it is difficult to apply this method to surfaces which involve microscopic asperities (except when one utilizes the complex multi-scale approach), an attempt is made in the present work to utilize asperities of larger size to examine the resulting stresses. Thus, the analyses are carried out in four different ways of representing the contact zone, namely, Contact without surface roughness peaks in 2D representation, 3D contact without surface roughness Peaks and contact with surface roughness peaks.

The analysis is carried out by using the code, ANSYS Rel 13.0. The boundary Conditions are as follows. As Work piece is fixed in chuck and live centre at ends, displacement is zero in UX direction. The load is applied on bottom surface of contact model. The contact between the roller and the workpiece is created using contact elements. Three loading passes are used in these analyses as per experimental data. For this purpose, the data obtained after each pass are taken as initial state of the workpiece and the analysis proceeded further.

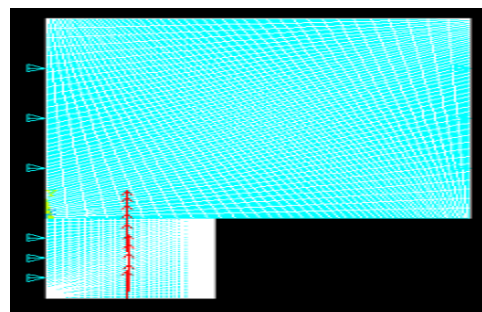


Fig. 5.: Loading diagram for the 2D model Without surface roughness peaks.

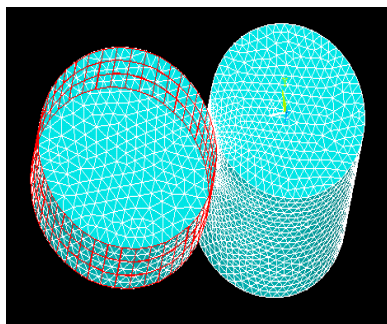


Fig:6. Loading diagram for 3D model without Surface roughness peaks.

| Sl. no | Force (N) | Contact stress | | | Contact width | | |
|--------|-----------|----------------|-----------------|--------|---------------|-----------------|------------------------|
| | | Hertz | Single asperity | Boresi | Hertz | Single asperity | Boresi |
| 1 | 50 | 106 | 107.868 | 78.41 | 0.0120 | 0.012 | 8.601×10^{-4} |
| 2 | 245 | 234.6 | 241.21 | 173.5 | 0.026 | 0.026 | 1.904×10^{-3} |
| 3 | 500 | 315 | 323.605 | 233.1 | 0.035 | 0.035 | 2.55×10^{-3} |

Table-2 .Comparison of contact width and contact stress for mild steel.

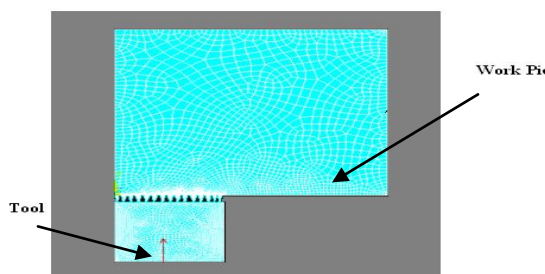


Fig:7 loading diagram for 2D model with Surface roughness peaks

3.0 RESULTS OBTAINED BY USING DIFFERENT THORIES

The results obtained by using the above theories and numerical methods are summarized in Table-2 below. It may be noted that among the various theories utilized, only the finite element method is capable of giving plasticity effects. This is because of the nature of formulations used in the Hertz, Boresi and single asperity methods.

Number of passes assumed in theories are 3.

| Type of FE model | Force (N) | Displacement | Von Mises Stress | Von Mises strain | Plastic strain |
|--------------------------|-----------|--------------|------------------|------------------|-----------------------------|
| Without peaks | 50 | 0.463e-03 | 94.434 | 0.606e-3 | Did not reach plastic stage |
| | 100 | 0.917e-3 | 188.799 | 0.001209 | Did not reach plastic stage |
| | 245 | 0.003143 | 190.098 | 0.001247 | 0.010588 |
| | 500 | 0.428e-03 | 96.937 | 0.601e-03 | - |
| With s/c roughness peaks | 25 | 0.517e-04 | 109.312 | 0.737e-03 | Did not reach plastic stage |
| | 50 | 0.103e-03 | 203.979 | 0.001372 | Did not reach plastic stage |
| | 100 | 0.214e-03 | 214.502 | 0.001179 | 0.012043 |
| 3D model without peaks | 50 | 0.001395 | 163.387 | 0.817e-3 | Did not reach plastic stage |
| | 245 | 0.007371 | 190.247 | 0.925e-3 | 0.007575 |
| | 500 | 0.017489 | 190.386 | 0.959e-3 | 0.043165 |

Table-3.2: Results of finite element analysis

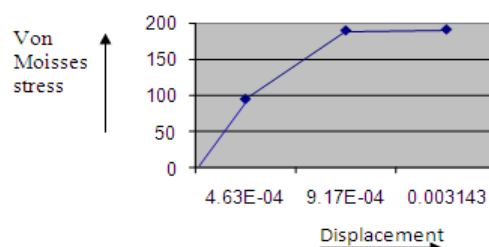


Fig: 8. Von misses stress Vs Displacement for Mild Steel

To show start of Plasticity as in Stress – Strain diagram.

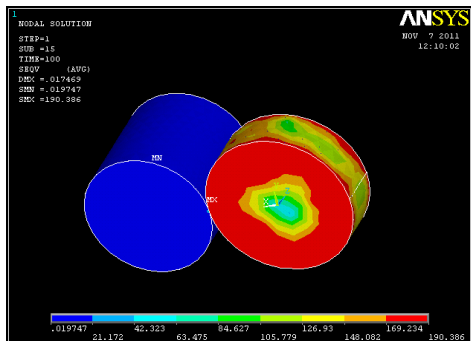


Fig: 9 Von Misses Stress for 3D contact Model.

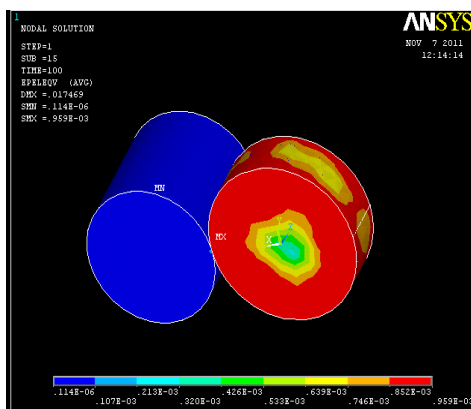


Fig:10 Von misses elastic strain for 3D Contact Model of 500N

4.0. DISCUSSION OF RESULTS

| Sl.no. | Force | Hertz | Single asperity | Boresi | Anslys results |
|--------|-------|--------|-----------------|--------|----------------|
| 1 | 50 | 106 | 107.868 | 78.41 | 94.434 |
| 2 | 245 | 234.64 | 241.21 | 173.56 | 190.098 |
| 3 | 500 | 315 | 323.605 | 233.13 | 96.937 |

Table: 1 Comparison of Contact Stress with Contact Model without peaks.

| Sl.no. | Force | Hertz | Single asperity | Boresi | Anslys results |
|--------|-------|--------|-----------------|--------|----------------|
| 1 | 50 | 106 | 107.868 | 78.41 | 163.387 |
| 2 | 245 | 234.64 | 241.21 | 173.56 | 190.247 |
| 3 | 500 | 315 | 323.605 | 233.13 | 190.386 |

Table: 2 Comparison of Contact Stress with 3DContact Model.

| Sl.no. | Force | Hertz | Single asperity | Boresi | Anslys results |
|--------|-------|--------|-----------------|--------|----------------|
| 1 | 50 | 106 | 107.868 | 78.41 | 203.979 |
| 2 | 245 | 234.64 | 241.21 | 173.56 | - |
| 3 | 500 | 315 | 323.605 | 233.13 | - |

Table: 3 Comparison of Contact Stress with Contact Model with peaks.

5.0. CONCLUSIONS

The Contact analysis Prove to about 10 to 15% variation in results. The Results Obtained indicates that Hertz Theory yields similar results to FEM Model. Discrepancies in comparison of results are due to the following reasons: i) Approximate Materials Properties used in simulation since text book values are different from Practice and ii) the modeling of contact by artificially creating peaks is inadequate since there are innumerable peaks to be modeled in a statistical manner. The best approach is to adopt multi-scale FEM methods.

REFERENCES

- 1) Jawalkar, C.S. and R. S. Walia., Study Of Roller Burnishing Process On En-8 Specimens Using Design Of Experiments Journal of Mechanical Engineering Research Vol. 1(1) pp. 038-045.
- 2) Eshwar Prasad,K., R.Murali Krishna., Experimental Investigation and Finite Element Analysis For The Study Of Residual Stresses In Roller Burnished Components. - International Journal of Applied Engineering Research ISSN0973-4562 Volume1.
- 3) El-Axi,M.H., An Investigation In To Roller Burnishing - International Journal of Machine Tools & Manufacture 40 (2000) 1603–1617.

- 4) Naga Malleswara Rao,J., A. Chennakesava Reddy and P.V. Rama Rao. Design And Fabrication Of New Type Of Dynamometer To Measure Radial Component Of Cutting Force And Experimental Investigation Of Optimum Burnishing Force In Roller Burnishing Process - Indian Journal of Science and Technology Vol. 3 No. 7 ISSN: 0974- 6846.
- 5) Lin, Y.C., S. W. Wang and H.-Y. Lai .,The Relationship Between Surface Roughness And Burnishing Factor In Burnishing Process - Int J Adv Manuf Technol (2004) 23: 666–671.
- 6) Bouzid Sa'ï , W. and K.Sa'I .,Finite Element Modeling Of Burnishing Of AISI 1042 steel - Int J Adv Manuf Technol 25: 460–465.
- 7) Ne'mat,M. and A. C. Lyons .,An Investigation of the Surface Topography of Ball Burnished Mild Steel and Aluminium - Int J Adv Manuf Technol 16:469–473.
- 8) Safwan M.A. and Al-Qawabah., Investigation of Roller Burnishing on Zamac5 Alloyed by Copper, Journal of Applied Sciences Research, 5(10): 1796-1801, 2009.
- 9) Hongyun Luo, Jianying Liu, LijiangWang and Qunpeng Zhong.,Investigation of the burnishing process with PCD tool on non-ferrous metals, Int J Adv Manufacturing Techno 25: 454–459.
- 10) El-Tayeb, N.S.M. K.O. Low, and P.V. Brevern .,Influence of roller burnishing contact width and burnishing orientation on surface quality and tribological behavior of Aluminum 6061, Journal of Materials Processing Technology 186 272–278.
- 11) G.G. Adams and M. Nosonovsky, Contact modeling- forces, Tribology International 33 (2000) 431–442
- 12) Borezi and R.J. Schmidt, "Advanced Mechanics of Materials" Sixth Edition, John Wiley & Sons, Inc., New York, 2003.